JOURNAL OF GUIDANCE, CONTROL, AND DYNAMICS
Vol. 27, No. 4, July–August 2004

Minimum-Energy Output Transitions for Linear Discrete-Time Systems: Flexible Structure Applications

Dhanakorn Iamratanakul, Hector Perez, and Santosh Devasia
University of Washington, Seattle, Washington 98195

This paper finds minimum-energy inputs to change the position of an output point, on a flexible structure, from one value to another. Current methods transform the output-transition problem into a state-to-state transition problem by constraining the initial and final states of the output transition, for example, to be rest (rigid-body) configurations of the flexible structure. However, the choice of the initial and final states can be ad hoc, and the resulting output-transition cost (input energy) might not be minimum. The contribution of this paper is the direct solution of the optimal output-transition problem; the problem is posed and solved for general linear discrete-time systems. The novelty of the proposed approach is that inputs are not applied just during the output-transition time interval; rather, inputs are also applied outside the output-transition time interval, that is, before the beginning of and after the end of the output-transition time interval. (These inputs are called pre- and postactuation.) The implications of using pre- and postactuation are illustrated by using an example of discrete-time flexible structure model, which consists of a flexible rod connecting two masses. Simulation results are presented, which show substantial reduction of output-transition costs with the use of the proposed method when compared to the use of the standard state-to-state transition approach.

I. Introduction

OPTIMAL design of maneuvers, to change the output from one value to another, arises in many flexible structure applications such as 1) positioning the endpoint of large-scale manipulators[1–4]; 2) positioning of read/write heads of disk-drive servo systems, which are relatively medium-scale flexible structures[5,6]; and 3) nanoscale positioning and manipulation using relatively small-scale piezoactuators, for example, Ref. 7. Additionally, we require that the output

Dhanakorn Iamratanakul received the B.S. degree in aerospace engineering from Kasetsart University, Thailand, in 1999 and the M.S. degree in aerospace engineering from the University of Southern California in 2000. He is currently in the Ph.D. program in Aeronautics and Astronautics at the University of Washington. His current research interests include inversion-based control theory, output-transition control, optimal control theory, and the control of complex distributed systems such as air traffic management. Student Member AIAA.

Hector Perez received the B.S. degree in electrical engineering in 1983, the M.S. degree in system engineering in 1991 from the Universidad Nacional de Colombia, and the Ph.D. degree in mechanical engineering from the University of Utah in 2002. He was a visiting student at the University of Washington in 2001–2002. He has been a research professor in the electronic engineering department at the Universidad Pontificia Bolivariana, Bucaramanga, Colombia since June 2002. His current research interests include inversion-based control theory, high-precision positioning systems, optimal control theory, image processing applied to control systems, and the application of the control technology in the Colombian industry. He is a member of ASME and IEEE.

Santosh Devasia received the B.S. from the Indian Institute of Technology, Kharagpur, India, in 1988, and the M.S. and Ph.D. degrees in mechanical engineering from the University of California at Santa Barbara in 1990 and 1993, respectively. He is an associate professor in the mechanical engineering department at the University of Washington, Seattle (since 2000). Previously, he had taught at the mechanical engineering department, University of Utah, Salt Lake City. His current research interests include inversion-based control theory, high-precision positioning systems for nanotechnology and biomedical applications, and the control of complex distributed systems such as air traffic management. Senior Member AIAA.

Received 31 October 2002; presented at the 2003 American Control Conference, Denver, CO, 4–6 June 2003; revision received 25 September 2003; accepted for publication 7 December 2003.

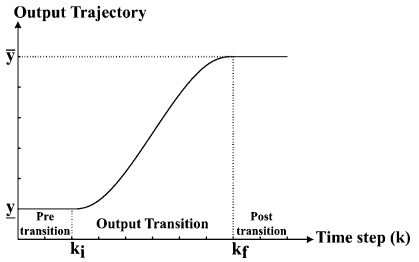

Fig. 1 Discrete-time output-transition problem: The output trajectory has to be maintained at a constant initial value $\underline{y}$ before the beginning of the output transition $[y(k) = \underline{y},\ k \le k_i]$ and at a constant final value $\bar{y}$ after the completion of the output transition $[y(k) = \bar{y},\ k \ge k_f]$.

(position of the output point on the flexible structure) be maintained at a constant value outside the output-transition time interval, as shown in Fig. 1. Maintaining the output constant outside of the transition time interval is critical to reduce the time lost to useful operations. For example, in the disk-drive application, the goal is to move the position of a read-write head from one track of a disk to another track; read and write operations cannot be performed (before and after the output transition) if the output position is not precisely maintained at the desired track. This problem of achieving output transitions is posed in the context of linear discrete-time systems. Formally, the output-transition problem is to find inputs that transfer (and maintain) the system output from an initial value $[y(k) = \underline{y}$ for all $k \le k_i]$ to a final value $[y(k) = \bar{y}$ for all $k \ge k_f]$ within a prescribed number of time steps $(k_f - k_i)$ where k_i and k_f denote the initial and final transition time steps. The main contribution of this paper is the direct solution of the optimal (minimum input-energy) output-transition problem. The method is applied to an illustrative flexible structure model, and simulation results are presented.

As opposed to the problem of changing the output point on a flexible structure, the problem of changing the complete configuration (i.e., the state) of a flexible structure has been well studied in literature, for example, Refs. 1–5, 8–10. These techniques, which solve the state-to-state transition problem (referred to as the state-transition problem), can also be used to find a solution to the output-transition problem. In particular, output transitions without residual vibrations can be obtained by requiring that the flexible system maneuver between equilibrium configurations (rigid-body rest configurations). (These rest states, $\underline{x}$ and $\bar{x}$, are chosen to result in the initial and final output values, $\underline{y}$ and $\bar{y}$, respectively.) Once the boundary states, at the beginning and end of the output transition, are chosen to be the rest states (i.e., $[x(k_i) = \underline{x},\ x(k_f) = \bar{x}]$), a solution to the output-transition problem can be found by solving the standard, minimum-energy, state-transition problem from the initial state $[x(k_i)]$ to the final state $[x(k_f)]$; this is referred to as the rest-to-rest state-transition approach (Refs. 3, 4, and 8). However, the solution found with this choice of the rest-to-rest boundary states $[x(k_i) = \underline{x},\ x(k_f) = \bar{x}]$ might not lead to optimal (minimum input energy) output transition. On the other hand, arbitrary choices of the boundary states $[x(k_i),\ x(k_f)]$ are also not acceptable; they might not allow the output to be maintained at a constant value after the completion of the output transition (i.e., without residual vibrations) for any choice of bounded inputs. Therefore, the standard optimal state-to-state transition approach cannot be used to directly solve the optimal output-transition problem.

The output-transition problem was previously addressed in Ref. 11, in which an inversion-based technique was used to plan an output transition along a prescribed output trajectory. However, the approach in Ref. 11 requires the user to specify (a priori) the set of acceptable output trajectories during the output transition (using polynomials); it is unclear how to choose such a set of output trajectories such that it includes the optimal output trajectory. Similar prespecification of a desired output trajectory is also needed in Ref. 12, which uses optimal filtering to achieve smooth transitions between output-trajectory segments in industrial positioning systems. In contrast, we do not require the prespecification of the output trajectory; rather, the best output trajectory is obtained as the result of the proposed optimization procedure. We do, however, use the stable inversion approach (as in Ref. 11) to find the preactuation $(k < k_i)$ inputs that maintain output tracking $(y = \underline{y})$ before initiating the output transition and similarly to find the postactuation $(k \ge k_f)$ inputs to maintain the output at the final value $\bar{y}$ after completing the output transition. The inversion-based approach, used to find pre- and postactuation inputs, is then integrated with standard optimal control approaches during the output-transition time interval (between time steps k_i and k_f) to solve the optimal output-transition problem. Thus, this method integrates the inversion-based control technique with the standard optimal control approach to solve the minimum-energy output-transition problem for discrete-time systems. (This extends results in Ref. 13 for continuous-time systems.)

In general, the proposed optimal output-transition approach uses both pre- and postactuation inputs to reduce the output-transition cost. (It is noted that the standard state-to-state transition approach uses neither pre- nor postactuation.) Preactuation input has to be applied to the system before the output transition is initiated; therefore, it requires preview information of an impending output transition. (The amount of required preview time is quantified in Ref. 14.) However, preactuation will not be applicable if such preview information of the desired output-transition is not available. For such cases, a modified output-transition approach is proposed that only uses postactuation (without preactuation). The implications of using (or not using) preactuation are investigated using an example discrete-time model of a flexible structure consisting of a flexible rod connecting two masses. The simulation results show significant reduction of the output-transition cost with the use of the proposed optimal output-transition method (with or without preactuation) when compared to the use of the standard approach that is based on state-to-state transition.

This paper is organized in the following format: The output-transition problem is posed in Sec. II. Section III presents a standard, minimum-energy, state-transition solution (SST) that solves the output-transition problem by choosing the initial and final transition states as equilibrium states. The optimal output-transition solution (OOT) is derived in Sec. IV. The application to flexible structure examples and the discussion of simulation results are in Sec. V. Our conclusions are in Sec. VI.

II. Problem Formulation

In the following, the flexible structure dynamics is modeled as a linear time-invariant system. Such linear models have been used in the past to represent dynamics of flexible structure systems. For example, linear models were used to represent the dynamics of flexible spacecraft in Refs. 1–3, to model the vibrational dynamics of disk-drive servosystems in Refs. 5 and 6 and to model the dynamics of flexible manipulators in Refs. 4, 7, 8, 9, 15, and 16. In particular, let the dynamics of the flexible structure be represented by a discrete-time model in the state-space form as

$$\begin{cases} x(k+1) = Ax(k) + Bu(k) \\ y(k) = Cx(k) \end{cases}, \qquad \forall k \in (-\infty, \infty) \qquad (1)$$

where the system state at time step k is $x(k) \in \Re^n$. Furthermore, it is assumed that the system is single input $u(k)$, single output $y(k)$ and controllable. Next, we consider the problem of changing the output position from one value to another within a finite time interval, called the output-transition time interval (i.e., the number of time steps to achieve the transition $k_f - k_i$). The output should be maintained constant (at the desired value) outside the output-transition time interval. Formally, the output-transition problem is defined as follows.

Definition 1: The output-transition problem is to find bounded input-state trajectories $[u(\cdot), x_{\text{ref}}(\cdot)]$ that satisfy the system equations in Eq. (1), that is,

$$\begin{cases} x_{\text{ref}}(k+1) = Ax_{\text{ref}}(k) + Bu(k) \\ y_{\text{ref}}(k) = Cx_{\text{ref}}(k) \end{cases}, \qquad \forall k \in (-\infty, \infty) \qquad (2)$$

and the following two conditions:

1) The output-transition condition is one where the output is transferred from the initial value $\underline{y}$ to the final value $\bar{y}$ within the output-transition time interval $[k_i, \overline{k}_f]$ and is maintained constant at the desired value before and after the output transition, that is,

$$y_{\text{ref}}(k) = \underline{y} = C\underline{x} \qquad \text{for} \qquad \forall k \le k_i$$
$$y_{\text{ref}}(k) = \bar{y} = C\bar{x} \qquad \text{for} \qquad \forall k \ge k_f \tag{3}$$

where k_i and k_f denote the initial and final transition time steps, respectively. Furthermore, $\underline{x}$ and $\bar{x}$ denote the desired initial and final equilibrium rigid-body configurations (i.e., the states $\underline{x} = A\underline{x}$ and $\bar{x} = A\bar{x}$).

2) The delimiting state condition is one where the state approaches the equilibrium states as time goes to (plus or minus) infinity, that is,

$$x_{\text{ref}}(k) \to \underline{x} \qquad \text{as} \qquad k \to -\infty$$
$$\text{and} \qquad x_{\text{ref}}(k) \to \bar{x} \qquad \text{as} \qquad k \to \infty \tag{4}$$

Next, we state the optimal output-transition problem.

Definition 2: The OOT (minimum-energy) problem is to find bounded input-state trajectories $[u(\cdot), x_{\text{ref}}(\cdot)]$ that solve the output-transition problem (definition 1) and minimize the following input-energy cost function:

$$J := \sum_{k=-\infty}^{\infty} [u(k)]^2 \tag{5}$$

III. SST Solution

The output-transition problem can be indirectly solved by converting the problem into a state-transition problem. The output-transition condition [Eq. (3)] and the delimiting state condition [Eq. (4)] can be satisfied by constraining all of the states before and after the output transition to be the equilibrium states. Formally, we redefine the conditions [Eqs. (3) and (4)] for the output-transition problem as follows:

The state-transition condition is

$$x(k) = \underline{x} \qquad \text{for} \qquad \forall k \le k_i$$
$$\text{and} \qquad x(k) = \bar{x} \qquad \text{for} \qquad \forall k \ge k_f \tag{6}$$

For controllable systems, there exists an input that can achieve the state transition from any initial state $x(k_i)$ to any final state $x(k_f)$ provided the following assumption is true.

Assumption 1: The length of output-transition time interval is greater than the number of states (n) in the discrete-time system [Eq. (1)]. □

The input to achieve the state transition [from $x(k_i)$ to $x(k_f)$] is not, however, unique; a particular input can be selected using an optimization criterion (e.g., minimum-energy criterion, as in this paper). A state-to-state solution to the output-transition problem (definition 1) using the minimum-energy criterion is given in the following lemma.

Lemma 1: Let assumption 1 be true. Then, given the boundary states ($\{x(k_i), x(k_f)\}$), the minimum-energy control input that transfers the system in Eq. (1) from the initial state $x(k_i)$ to the final state $x(k_f)$ is given by

$$u^*_{\text{sst}}(k) := B^T (A^T)^{k_f - k - 1} G^{-1}_{k_i, k_f} \Delta_x, \qquad k_i \le k < k_f$$
$$:= 0, \qquad \text{otherwise} \tag{7}$$

where G_{k_i,k_f} is the invertible controllability grammian defined by

$$G_{k_i,k_f} := \sum_{k=k_i}^{k_f - 1} A^{k_f - k - 1} B B^T (A^T)^{k_f - k - 1} \tag{8}$$

and Δ_x is the transition state difference,

$$\Delta_x := \Delta_x[k_i, x(k_i), k_f, x(k_f)] = x(k_f) - A^{k_f - k_i} x(k_i) \tag{9}$$

Furthermore, the cost function [Eq. (5)] when using the optimal state-transition control input [Eq. (7)] is given by

$$J^*_{\text{sst}} = \Delta_x^T G^{-1}_{k_i,k_f} \Delta_x \tag{10}$$

Proof: Because we consider the transition from the state $x(k_i)$ at the time step k_i to the state $x(k_f)$ at the time step k_f, the applied input is zero during the pretransition ($k \le k_i$) and posttransition ($k \ge k_f$). Therefore, the cost function (5) is reduced to the input energy required during the output-transition time interval, that is,

$$J = \sum_{k=k_i}^{k_f - 1} [u(k)]^2 \tag{11}$$

The optimal control input $u^*_{\text{sst}}(k)$ that minimizes the cost function (11) subject to the state-transition condition (6) can be obtained by using a standard linear-quadratic optimal control technique, for example, see Ref. 17, pp. 47–49, and Ref. 16. The associated optimal cost is obtained by substituting the optimal state-transition control input to the cost function [Eq. (11)]. □

Output transition using the SST approach: A solution to the output-transition problem (definition 1) can be found using the state-transition approach by finding the minimum-energy input to achieve the state transition from the initial state $[x(k_i) = \underline{x}]$ to the final transition state $[x(k_f) = \bar{x}]$ using Lemma 1. Note that the boundary states $\{[x(k_i), x(k_f)]\}$ for the transition are equilibrium states, and so the transition state difference (9) can be rewritten as

$$\Delta_x[k_i, \underline{x}, k_f, \bar{x}] = \bar{x} - A^{k_f - k_i}\underline{x} = \bar{x} - \underline{x}$$

The input is then found using this transition state difference ($\Delta_x = \Delta_x[k_i, \underline{x}, k_f, \bar{x}]$) in Eq. (7). The solution to output-transition problem achieved by using the minimum-energy state-to-state transition approach is referred to, in this paper, as the SST solution.

IV. OOT Solution

We begin by identifying the set of possible boundary states $\{x(k_i), x(k_f)\}$ that allows the output to be maintained at constant value before and after the output-transition time interval, that is, compatible with the output-transition condition (3). This is done in two steps. First the original system (1) is converted into the output-tracking form (or normal form, see Ref. 18). Second, the control inputs required before the initiation of the output transition (preactuation) and after the completion of the output transition (postactuation) are found. Once the set of possible boundary states $\{x(k_i), x(k_f)\}$ compatible with the output-transition condition (3) is identified, the optimal boundary states are found (from this set) and used to solve the minimum-energy output-transition problem.

A. Output-Tracking Form

The output-tracking form decouples the system states into 1) those that directly influence the output and 2) unobservable internal states. The output-tracking form depends on the delay order of the system,[19] which is the difference between the number of poles and the number of zeros of the discrete-time system. The delay order in discrete-time systems is similar to the relative degree in continuous-time systems.

Remark 1: A delay order r implies that there is an r-step delay before the output changes in response to an input applied at time step k, that is, the input $u(k)$ will only affect the output y at time step $k + r$ and after (but not the output before time step $k + r$). □

Assumption 2: The discrete-time system [Eq. (1)] has a delay order r. □

1. Input and Coordinate Transformations

From the definition of delay order, the r-forward time-shift output equation can be written explicitly in terms of the input as[19]

$$y(k+r) = CA^r x(k) + CA^{r-1}Bu(k) \tag{12}$$

where $CA^{r-1}B \neq 0$. Then the unique inverse control input

$$u_{\text{inv}}(k) := (1/CA^{r-1}B)[y_d(k+r) - CA^r x(k)] \tag{13}$$

maintains exact output tracking [i.e., $y(k+r) = y_d(k+r)$], which can be verified by substituting the input from Eq. (13) into Eq. (12). Assumption 2 also implies that there exists a coordinate transformation matrix, $T_{\xi\eta}$, whose first r rows are chosen as $C, CA, CA^2, \ldots, CA^{r-1}$, and the remaining $n-r$ rows are chosen such that the matrix $T_{\xi\eta}$ is invertible, that is,

$$T_{\xi\eta} := \begin{bmatrix} C \\ CA \\ \vdots \\ \hline CA^{r-1} \\ \hline T_\eta \end{bmatrix} \tag{14}$$

The set $\{C, CA, \ldots, CA^{r-1}\}$ is linearly independent; therefore, we can always find T_η [in Eq. (14)] such that $T_{\xi\eta}$ is invertible (see Ref. 19). The transformation matrix $T_{\xi\eta}$ partitions the state $x(k)$ into two components: 1) the first r terms are the output and its $r-1$ future values (denoted by ξ), and 2) the remaining components are called the internal state of the system (denoted by η), that is,

$$T_{\xi\eta}x(k) = \begin{bmatrix} \xi(k) \\ \hline \eta(k) \end{bmatrix} := \begin{bmatrix} y(k) \\ y(k+1) \\ \vdots \\ \hline y(k+r-1) \\ \hline \eta(k) \end{bmatrix} \tag{15}$$

2. Internal Dynamics

Applying the coordinate transformation $T_{\xi\eta}$ [Eq. (14)] and the inverse control law [Eq. (13)] to the original system [Eq. (1)], we have

$$\begin{aligned}
\begin{bmatrix} \xi(k+1) \\ \eta(k+1) \end{bmatrix} &= T_{\xi\eta}AT_{\xi\eta}^{-1}\begin{bmatrix} \xi(k) \\ \eta(k) \end{bmatrix} + T_{\xi\eta}Bu_{\text{inv}}(k) \\
&= T_{\xi\eta}AT_{\xi\eta}^{-1}\begin{bmatrix} \xi(k) \\ \eta(k) \end{bmatrix} \\
&\quad + T_{\xi\eta}B\left\{\frac{1}{CA^{r-1}B}[y_d(k+r) - CA^r x(k)]\right\} \\
&= \left(T_{\xi\eta}AT_{\xi\eta}^{-1} - \frac{T_{\xi\eta}BCA^rT_{\xi\eta}^{-1}}{CA^{r-1}B}\right)\begin{bmatrix} \xi(k) \\ \eta(k) \end{bmatrix} \\
&\quad + \frac{T_{\xi\eta}B}{CA^{r-1}B}y_d(k+r) \\
&:= \begin{bmatrix} A_\xi & 0 \\ A_{\eta\xi} & A_\eta \end{bmatrix}\begin{bmatrix} \xi(k) \\ \eta(k) \end{bmatrix} + \begin{bmatrix} B_{\xi\xi} \\ B_{\eta\eta} \end{bmatrix} y_d(k+r)
\end{aligned}$$

where the matrix A_η has dimension $(n-r)\times(n-r)$, r is the delay order, and n is the number of the states of the system. The preceding equations can be rewritten in the output-tracking form as

$$\xi(k+1) = \xi_d(k+1) \tag{16}$$

$$\begin{aligned}
\eta(k+1) &= A_\eta\eta(k) + \begin{bmatrix} A_{\eta\xi} & B_{\eta\eta} \end{bmatrix}\mathbb{Y}_d(k) \\
&:= A_\eta\eta(k) + B_\eta\mathbb{Y}_d(k)
\end{aligned} \tag{17}$$

where the output sequence

$$\mathbb{Y}_d(k) := \begin{bmatrix} \xi_d(k) \\ y_d(k+r) \end{bmatrix}$$

represents the vector of desired values of the output. In the preceding notation, the variables with a subscript d denote the known (desired) value. The last equation [Eq. (17)] is called the internal dynamics of the system.

We will assume (without loss of generality) that the internal dynamics [Eq. (17)] has the following decoupled form:

$$\begin{aligned}
\eta(k+1) := \begin{bmatrix} \eta_s(k+1) \\ \eta_u(k+1) \\ \eta_c(k+1) \end{bmatrix} &= \begin{bmatrix} A_s & 0 & 0 \\ 0 & A_u & 0 \\ 0 & 0 & A_c \end{bmatrix}\begin{bmatrix} \eta_s(k) \\ \eta_u(k) \\ \eta_c(k) \end{bmatrix} \\
&\quad + \begin{bmatrix} B_s \\ B_u \\ B_c \end{bmatrix}\mathbb{Y}_d(k)
\end{aligned} \tag{18}$$

where the internal state is decoupled into strictly stable (η_s), unstable (η_u), and center (η_c) subspaces. In the preceding decoupled equations, the eigenvalues of A_s are the minimum-phase zeros of system (1) that are inside the unit circle in the complex plane, the eigenvalues of A_u are the nonminimum-phase zeros located outside the unit circle, and the eigenvalues of A_c are the zeros located on the unit circle. Furthermore, the inverse control law (13) can be rewritten in terms of the decoupled internal states and the known output sequence $\mathbb{Y}_d(k)$ [using the transformation $T_{\xi\eta}$ in Eq. (14)] as

$$\begin{aligned}
u_{\text{inv}}(k) &= \frac{1}{CA^{r-1}B}y_d(k+r) - \frac{CA^rT_{\xi\eta}^{-1}}{CA^{r-1}B}\begin{bmatrix} \xi_d(k) \\ \eta_s(k) \\ \eta_u(k) \\ \eta_c(k) \end{bmatrix} \\
&:= \frac{1}{CA^{r-1}B}y_d(k+r) + U_\xi\xi_d(k) \\
&\quad + U_s\eta_s(k) + U_u\eta_u(k) + U_c\eta_c(k) \\
&= U_s\eta_s(k) + U_u\eta_u(k) + U_c\eta_c(k) \\
&\quad + \begin{bmatrix} U_\xi & \dfrac{1}{CA^{r-1}B} \end{bmatrix}\begin{bmatrix} \xi_d(k) \\ y_d(k+r) \end{bmatrix} \\
&:= U_s\eta_s(k) + U_u\eta_u(k) + U_c\eta_c(k) + U_y\mathbb{Y}_d(k)
\end{aligned} \tag{19}$$

Remark 2: The inverse control law [Eq. (19)] and the transformation $T_{\xi\eta}$ make the internal states $\eta(k)$ unobservable; therefore, changes in the internal states will not affect the output. □

Remark 3: The inputs applied at time step $k_i - r$ and after do not affect the output until the beginning of the output-transition time step k_i (from the delay order assumption 2 and remark 1). Therefore, the inverse input [Eq. (19)] to maintain the output at a constant value $[y(k) = \underline{y}$ for all $k \leq k_i)]$ is only required before time step $k_i - r + 1$ during the pretransition. □

B. Preactuation ($k \leq k_i - r$)

During pretransition, the output has to be maintained at a constant value $[y(k) = \underline{y}$ for all $k \leq k_i]$. The only preactuation input that can maintain such a constant output trajectory is the inversion-based input [Eq. (19)]. Because the output trajectory during the pretransition interval is known (equal to $\underline{y}$), the inversion-based input [Eq. (19)] is completely determined by the choice of internal state. In particular, if the boundary internal state $\eta(k_i - r + 1)$ at time step $k_i - r + 1$ is specified then the internal state can be obtained by solving the internal dynamics [Eq. (18)] recursively backward in time, starting at the beginning of the output transition (time step $k_i - r + 1$). The internal state is unobservable under the inverse control law (Remark 2); therefore, the preactuation input computed with any

choice of the boundary internal state $\eta(k_i - r + 1)$ always satisfies the output-transition condition [Eq. (3)]. However the preactuation input (to maintain the constant output) tends to be unbounded for arbitrary choices of the internal state $\eta(k_i - r + 1)$. Thus, there is a need to identify the set of acceptable boundary internal states at the beginning of the output transition (time step $k_i - r + 1$), for which we can find bounded preactuation inputs to satisfy, both, the output-transition condition and the delimiting-state condition.

The next lemma quantifies the set of acceptable boundary internal states at the beginning of the output transition (time step $k_i - r + 1$). In particular, the lemma shows that the stable η_s and center η_c components of the internal dynamics at the beginning of the output transition must be chosen such that they correspond to the values of the initial equilibrium configuration $\underline{x}$. Thus, the only flexibility in the choice of the boundary internal states at the beginning of the output transition is in the value of the unstable component $\eta_u(k_i - r + 1)$ of the internal dynamics. Therefore, the preactuation input for the output-transition problem can be uniquely defined in terms of the unstable component $\eta_u(k_i - r + 1)$. Furthermore, the lemma shows that the cost of using preactuation input is quadratic in the unstable, internal-state component $\eta_u(k_i - r + 1)$.

Lemma 2: The preactuation input that satisfies the output-tracking conditions [Eqs. (3), and (4) in definition 1] is uniquely specified in terms of the choice of the unstable internal-state component $\eta_u(k_i - r + 1)$ and is given by

$$u_{\text{pre}}(k) := U_u A_u^{-(k_i - k - r + 1)}[\eta_u(k_i - r + 1) - \underline{\eta}_u] \qquad \forall k \in (-\infty, k_i - r] \quad (20)$$

where $\underline{\eta} = T_\eta \underline{x}$. Furthermore, the cost associated with this preactuation input $u_{\text{pre}}(k)$ is equal to

$$J_{\text{pre}} := [\eta_u(k_i - r + 1) - \underline{\eta}_u]^T W_{\text{pre}}[\eta_u(k_i - r + 1) - \underline{\eta}_u] \quad (21)$$

where

$$W_{\text{pre}} := \sum_{k=0}^{\infty} \left(A_u^T\right)^{-(k+1)} U_u^T U_u A_u^{-(k+1)} \quad (22)$$

is a real symmetric matrix that can be computed by solving the discrete-time algebraic Lyapunov equation

$$\left(A_u^{-1}\right)^T W_{\text{pre}} A_u^{-1} - W_{\text{pre}} + \left(A_u^{-1}\right)^T U_u^T U_u A_u^{-1} = 0 \quad (23)$$

Proof: See Appendix. □

C. Postactuation ($k \geq k_f$)

The postactuation input is obtained by using procedures similar to that used in the preceding subsection for finding the preactuation input. The next lemma quantifies the set of acceptable boundary internal states at the end of the output transition (time step k_f). In particular, the lemma shows that the unstable η_u and center η_c components of the internal dynamics at the beginning of the output transition must be chosen such that they correspond to the values of the final equilibrium configuration $\bar{x}$. Thus, the only flexibility in the choice of the boundary internal states at the end of the output transition is in the value of the stable component $\eta_s(k_f)$ of the internal dynamics. Therefore, the postactuation input for the output-transition problem can be uniquely defined in terms of the stable component $\eta_s(k_f)$. Furthermore, the lemma shows that the cost of using postactuation input is quadratic in the stable, internal-state component $\eta_s(k_f)$.

Lemma 3: The postactuation input that satisfies the output-tracking conditions [Eqs. (3) and (4) in definition 1] is uniquely specified in terms of the choice of the stable internal-state component $\eta_s(k_f)$ and is given by

$$u_{\text{post}}(k) := U_s A_s^{k - k_f}[\eta_s(k_f) - \bar{\eta}_s] \qquad \forall k \in [k_f, \infty) \quad (24)$$

where $\bar{\eta} = T_\eta \bar{x}$. Furthermore, the cost associated with this postactuation input $u_{\text{post}}(k)$ is equal to

$$J_{\text{post}} := [\eta_s(k_f) - \bar{\eta}_s]^T W_{\text{post}}[\eta_s(k_f) - \bar{\eta}_s] \quad (25)$$

where

$$W_{\text{post}} := \sum_{k=0}^{\infty} \left(A_s^T\right)^k U_s^T U_s A_s^k \quad (26)$$

is a real symmetric matrix that can be computed by solving the discrete-time algebraic Lyapunov equation

$$A_s^T W_{\text{post}} A_s - W_{\text{post}} + U_s^T U_s = 0 \quad (27)$$

Proof: The proof is similar to the proof of Lemma 2 and is, therefore, omitted. □

Remark 4: Lemma 2 implies that the only freedom in the state at the initiation of output-transition $x(k_i - r + 1)$ is in the choice of the unstable internal-state component $\eta_u(k_i - r + 1)$ (see proof of Lemma 2). Similarly, Lemma 3 implies that the only freedom in the state at the completion of output transition $x(k_f)$ is in the choice of the stable internal-state component $\eta_s(k_f)$. Therefore, a particular choice of these unconstrained subspaces $\{\eta_u(k_i - r + 1), \eta_s(k_f)\}$ completely specifies the boundary states $\{x(k_i - r + 1), x(k_f)\}$ at the beginning and end of the output transition. □

Definition 3: The output-transition boundary condition Ψ is the component of the state (in the output tracking coordinate), at the initiation and completion of the output transition, that can be varied while satisfying the conditions for the output transition (see remark 4) and is defined as

$$\Psi := \begin{bmatrix} \eta_s^T(k_f) & \eta_u^T(k_i - r + 1) \end{bmatrix}^T \quad (28)$$

Remark 5: In the standard state-transition solution (7), the output-transition boundary condition Ψ is determined by the equilibrium states, that is, $\Psi_{\text{sst}} = [\eta_s^T(k_f) \;\; \eta_u^T(k_i - r + 1)]^T = [\bar{\eta}_s^T \;\; \underline{\eta}_u^T]^T := \tilde{\Psi}$. □

D. Transition Interval ($k_i - r < k < k_f$)

The choice of the output-transition boundary condition Ψ [Eq. (28)] specifies the preactuation and postactuation inputs (and associated costs); however, it does not specify the input during the output-transition time interval. The input needed during the output-transition time interval can be optimally found by using the SST technique (see Lemma 1) with the initial and final states chosen as

$$\begin{aligned} x(k_i - r + 1) &= T_{\xi\eta}^{-1}\begin{bmatrix} \underline{\xi}^T & \underline{\eta}_s^T & \eta_u(k_i - r + 1)^T & \underline{\eta}_c^T \end{bmatrix}^T \\ &:= \left[\Phi_\xi \middle| \Phi_{\eta_s} \middle| \Phi_{\eta_u} \middle| \Phi_{\eta_c}\right]\begin{bmatrix} \underline{\xi}^T & \underline{\eta}_s^T & \eta_u(k_i - r + 1)^T & \underline{\eta}_c^T \end{bmatrix}^T \\ x(k_f) &= T_{\xi\eta}^{-1}\begin{bmatrix} \bar{\xi}^T & \eta_s(k_f)^T & \bar{\eta}_u^T & \bar{\eta}_c^T \end{bmatrix}^T \end{aligned} \quad (29)$$

where $[\underline{\xi}^T \;\; \underline{\eta}_s^T \;\; \underline{\eta}_u^T \;\; \underline{\eta}_c^T]^T = T_{\xi\eta} x$, and $[\bar{\xi}^T \;\; \bar{\eta}_s^T \;\; \bar{\eta}_u^T \;\; \bar{\eta}_c^T]^T = T_{\xi\eta}\bar{x}$. The associated minimum input-energy $J_{\text{sst}}^*(k_i - r + 1, k_f, \Psi)$ during the output-transition time interval can be written in terms of the boundary condition Ψ as [using Eq. (10)]

$$J_{\text{tran}} := J_{\text{sst}}^*(k_i - r + 1, k_f, \Psi) = \Delta_\Psi^T \hat{G}_{k_i, k_f}^{-1} \Delta_\Psi \quad (30)$$

where

$$\hat{G}_{k_i, k_f} = \sum_{k=k_i - r + 1}^{k_f - 1} A^{k_f - k - 1} B B^T (A^T)^{k_f - k - 1}$$

and the final state difference Δ_Ψ is redefined in terms of the boundary condition Ψ as [from Eq. (9)]

$$\begin{aligned} \Delta_\Psi &= \Delta_x[k_i - r + 1, x(k_i - r + 1), k_f, x(k_f)] \\ &= x(k_f) - A^{k_f - k_i + r - 1} x(k_i - r + 1) \\ &:= H_1 \hat{f} + H_2 \Psi \end{aligned} \quad (31)$$

where

$$H_1 := \left[\Phi_\xi | \Phi_{\eta_u} \middle| \Phi_{\eta_c} \middle| -\Gamma_\xi | -\Gamma_{\eta_s} \middle| -\Gamma_{\eta_c}\right]$$

$$H_2 := \left[\Phi_{\eta_s} \middle| -\Gamma_{\eta_u}\right]$$

$$\left[\Gamma_\xi | \Gamma_{\eta_s} \middle| \Gamma_{\eta_u} \middle| \Gamma_{\eta_c}\right] := A^{k_f - k_i - r + 1} T_{\xi\eta}^{-1}$$

$$\hat{f} := \left[\bar{\xi}^T \quad \bar{\eta}_u^T \quad \bar{\eta}_c^T \quad \underline{\xi}^T \quad \underline{\eta}_s^T \quad \underline{\eta}_c^T\right]^T$$

E. Optimal Output Transition

The input energy needed for output transition with a specified output-transition boundary condition Ψ (definition 3) can be obtained by substituting the pretransition cost [Eq. (21)], the posttransition cost [Eq. (25)], and the transition cost [Eq. (30)] into the input cost [Eq. (5)] as follows:

$$J_{\text{oot}}(\Psi) = \sum_{k=-\infty}^{\infty} [u(k)]^2 = J_{\text{pre}} + J_{\text{tran}} + J_{\text{post}}$$

$$:= \Psi^T \Lambda \Psi - 2\Psi^T b + c \tag{32}$$

where

$$\Lambda := \begin{bmatrix} W_{\text{post}} & 0 \\ 0 & W_{\text{pre}} \end{bmatrix} + H_2^T \hat{G}_{k_i,k_f}^{-1} H_2$$

$$b := \begin{bmatrix} W_{\text{post}} \bar{\eta}_s \\ W_{\text{pre}} \underline{\eta}_u \end{bmatrix} - H_2^T \hat{G}_{k_i,k_f}^{-1} H_1 \hat{f}$$

$$c := \bar{\eta}_s^T W_{\text{post}} \bar{\eta}_s + \underline{\eta}_u^T W_{\text{pre}} \underline{\eta}_u + \hat{f}^T H_1^T \hat{G}_{k_i,k_f}^{-1} H_1 \hat{f}$$

Note that the input-energy needed for output transition [Eq. (32)] is quadratic in terms of the specified output-transition boundary condition Ψ. The optimal value for the output-transition boundary condition Ψ is found in the next theorem, which solves the OOT problem.

Theorem 1: Let assumptions 1 and 2 be true. Then, the minimum-energy output-transition problem (definition 2) always has a solution described in the following:

1) The optimal boundary condition Ψ that minimizes the cost function [Eq. (32)] is given by

$$\Psi^* = \begin{bmatrix} \eta_s^* \\ \eta_u^* \end{bmatrix} = \begin{cases} \Lambda^{-1} b, & \text{if} \quad \Lambda \quad \text{is invertible} \\ \Lambda^\dagger b, & \text{otherwise} \end{cases} \tag{33}$$

where $\Lambda^\dagger$ is the pseudo (generalized)-inverse of Λ (Ref. 20).

2) The control input for the optimal output-transition problem is given as

$$u_{\text{oot}}^*(k) = \begin{cases} U_u A_u^{k-k_i+r-1} \left[\eta_u^* - \underline{\eta}_u\right] & \text{if} \quad k \le k_i - r \\ B^T (A^T)^{k_f-k-1} \hat{G}_{k_i,k_f}^{-1} \left[x^*(k_f) - A^{k_f-k_i+r-1} x^*(k_i - r + 1)\right] & \text{if} \quad k_i - r < k < k_f \\ U_s A_s^{k-k_f} \left[\eta_s^* - \bar{\eta}_s\right] & \text{if} \quad k \ge k_f \end{cases} \tag{34}$$

where the optimal boundary states for the output transition are

$$x^*(k_i - r + 1) = T_{\xi\eta}^{-1} \begin{bmatrix} \underline{\xi} \\ \underline{\eta}_s \\ \eta_u^* \\ \underline{\eta}_c \end{bmatrix}, \qquad \text{and} \qquad x^*(k_f) = T_{\xi\eta}^{-1} \begin{bmatrix} \bar{\xi} \\ \eta_s^* \\ \bar{\eta}_u \\ \bar{\eta}_c \end{bmatrix} \tag{35}$$

3) The optimal output-transition cost using the OOT input [Eq. (34)] is equal to

$$J_{\text{oot}}^* = \Psi^{*T} \Lambda \Psi^* - 2\Psi^{*T} b + c \tag{36}$$

Proof: The output-transition cost function [Eq. (32)] is quadratic in terms of the boundary condition Ψ; therefore, the optimal value for the boundary condition Ψ follows from the minimization of quadratic forms, see Theorem 1 in Ref. 13 and Theorem 4.2.1 in Ref. 20. The optimal output-transition input follows from Lemmas 1, 2, and 3. The associated optimal cost is obtained by substituting the optimal boundary condition Ψ^* into the output-transition cost function [Eq. (32)]. □

Remark 6: The optimal cost for output-transition problem [Eq. (36)] is always less than or equal to the optimal cost for the state-transition problem [Eq. (10)] because the OOT input minimizes the energy over all possible solutions to the output-transition problem (definition 1), which includes the solution from the SST approach (using $\Psi = \tilde{\Psi}$, see Remark 5). □

F. Optimal Output Transition Without Preactuation

In general, the proposed optimal output-transition approach uses both pre- and postactuation inputs to reduce the output-transition cost. Preactuation input has to be applied to the system before the output transition is initiated; therefore, it requires preview information of the impending output transition. However, the preactuation might not be applicable if such preview information of the desired output transition is not available (e.g., when immediate output transition is desired). For such cases, we require that the output transition begin with the initial transition state at the equilibrium (rest) state, that is, $x(k_i) = \underline{x}$. Then, the optimal output-transition approach can be constrained to only use postactuation, that is, by optimally choosing the stable component of the internal dynamics at the completion of the output transition $\eta_s(k_f)$. Therefore, the output-transition cost function [Eq. (32)] can be rewritten as

$$\tilde{J}[\eta_s(k_f)] := [\eta_s(k_f)]^T \tilde{\Lambda} [\eta_s(k_f)] - 2[\eta_s(k_f)]^T \tilde{b} + \tilde{c} \tag{37}$$

where

$$\tilde{\Lambda} := W_{\text{post}} + \tilde{H}_2^T G_{k_i,k_f}^{-1} \tilde{H}_2, \qquad \tilde{b} := W_{\text{post}} \bar{\eta}_s - \tilde{H}_2^T G_{k_i,k_f}^{-1} \tilde{H}_1 \tilde{f}$$

$$\tilde{c} := \bar{\eta}_s^T W_{\text{post}} \bar{\eta}_s + \tilde{f}^T \tilde{H}_1^T G_{k_i,k_f}^{-1} \tilde{H}_1 \tilde{f}$$

$$\tilde{f} := \left[\bar{\xi}^T \quad \bar{\eta}_u^T \quad \bar{\eta}_c^T \quad \underline{\xi}^T \quad \underline{\eta}_s^T \quad \underline{\eta}_u^T \quad \underline{\eta}_c^T\right]^T$$

$$\tilde{H}_1 := \left[\Phi_\xi | \Phi_{\eta_u} \middle| \Phi_{\eta_c} \middle| -\tilde{\Gamma}\right], \qquad \tilde{H}_2 := \Phi_{\eta_s}, \qquad \tilde{\Gamma} := A^{k_f - k_i} T_{\xi\eta}^{-1}$$

where the grammian G_{k_i,k_f}^{-1} is given by Eq. (8). Next, the solution to the OOT problem without preactuation is provided in the following lemma.

Lemma 4: The optimal stable internal state $\eta_s(k_f)$ that minimizes the output-transition cost without preactuation [Eq. (37)] is then given by

$$\tilde{\eta}_s^*(k_f) = \begin{cases} \tilde{\Lambda}^{-1} \tilde{b}, & \text{if} \quad \tilde{\Lambda} \quad \text{is invertible} \\ \tilde{\Lambda}^\dagger \tilde{b}, & \text{otherwise} \end{cases} \tag{38}$$

where $\tilde{\Lambda}^\dagger$ is the pseudo (generalized)-inverse of $\tilde{\Lambda}$. The optimal control input, for the output-transition problem without preactuation, is

given by

$$\tilde{u}^*_{\text{oot}}(k) = \begin{cases} 0 & \text{if} \quad k < k_i \\ B^T (A^T)^{k_f - k - 1} G^{-1}_{k_i, k_f} [x^*(k_f) - \underline{x}] & \text{if} \quad k_i \le k < k_f \\ U_s A_s^{k - k_f} \left[\tilde{\eta}^*_s(k_f) - \bar{\eta}_s \right] & \text{if} \quad k \ge k_f \end{cases} \tag{39}$$

where the optimal final transition states are computed from

$$\tilde{x}^*(k_f) = T^{-1}_{\xi\eta} \begin{bmatrix} \bar{\xi}^T & \tilde{\eta}^*_s(k_f)^T & \bar{\eta}^T_u & \bar{\eta}^T_c \end{bmatrix}^T$$

Proof: This follows from arguments similar to those in the proof of Theorem 1 because the cost without preactuation [Eq. (37)] has the same quadratic form as in Theorem 1 [Eq. (32)]. □

Remark 7: Given the initial state $x(k_i) = \underline{x}$ (as in the preceding Lemma 4), the optimal input, which ensures that the output reaches the final value $y(k_f) = \bar{y}$ at the end of output transition, can be solved by using standard optimal control, for example, Ref. 17. This procedure does not require that the output be maintained at a constant value outside the output-transition time interval. Therefore, this approach will not guarantee that the unstable internal state $[\eta_u(k_f)]$ and the center internal state $[\eta_c(k_f)]$ will be at the equilibrium configuration at the end of output transition (see Remark 4), and a bounded input cannot be found to maintain the output at a constant value after the completion of the output transition. □

V. Example Flexible-Structure Model: Simulation Results and Discussion

In this section, the OOT approach is demonstrated using an example flexible-structure model, which consists of two masses connected by a flexible coupling (see Fig. 2). (The computer code to generate the following simulations is available by authors upon request.) The two-mass/flexible-coupling model has been widely used as a benchmark problem to study the control performance for flexible structure systems (e.g., Refs. 8, 9, and 21). In contrast to modeling the flexible coupling simply as a lumped spring and a damper element (which results in a minimum-phase continuous-time model), the flexible coupling in this example is modeled as a continuum rod. The flexible rod dynamics includes the wave-propagation effect between the noncollocated input and output; as a result, the system model exhibits nonminimum-phase behavior that is characteristic of continuum models of flexible structures with noncollocated inputs and outputs (e.g., see Refs. 15 and 22).

A. System Description

We consider two masses linked by a flexible rod, as shown in Fig. 2. The input $u(t)$ is the force applied to the mass m_2 on the left side of the rod, and the output is the displacement of the mass m_1 on the right side of the rod. The goal is to change the output (the position of the mass m_1) by one unit length with minimum energy effort. The dynamics of the system, modeled as a simplified two-node axial rod (using finite element method, e.g., see Ref. 23), can be represented by

$$\{[M^l] + [M^r]\}\ddot{\mathbb{X}}(t) + [C^r]\dot{\mathbb{X}}(t) + [K^r]\mathbb{X}(t) = \begin{bmatrix} 0 \\ 1 \end{bmatrix} u(t) \tag{40}$$

$$[M^l] := \begin{bmatrix} m_1 & 0 \\ 0 & m_2 \end{bmatrix}, \qquad [M^r] := m_r \begin{bmatrix} 2 & 1 \\ 1 & 2 \end{bmatrix}$$

$$[K^r] := k_r \begin{bmatrix} 1 & -1 \\ -1 & 1 \end{bmatrix} \quad \text{and} \quad [C^r] := c_r \begin{bmatrix} 1 & -1 \\ -1 & 1 \end{bmatrix}$$

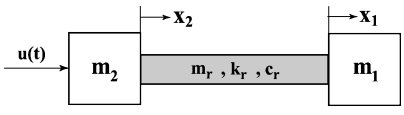

Fig. 2 Two masses connected by a flexible coupling: The flexible coupling is modeled as a continuum rod.

where the vector $\mathbb{X}(t) := [x_1(t) \;\; x_2(t)]^T$ is the position vector of the two lumped masses attached at both ends of the rod and the matrix $[M^l]$ is the diagonal mass-matrix term associated with the endpoint masses m_1 and m_2. The matrix $[M^r]$ is the mass-matrix term representing the distributed mass of the rod, the matrix $[K^r]$ is the stiffness matrix, and the matrix $[C^r]$ is the structural damping matrix. The parameter m_r represents the mass-matrix coefficient of the rod, that is, $m_r = (\rho_r A_r l_r)/6$, where ρ_r, A_r, and l_r represent density, cross-sectional area, and length of the flexible rod, respectively. The parameter k_r represents the stiffness coefficient of the flexible rod ($k_r = A_r E_r / l_r$, where E_r is the elasticity modulus of the rod). The damping constant c_r is proportional to the stiffness k_r, that is, $c_r = \alpha_r k_r$, where α_r is the damping factor of the flexible rod. In the simulations, the system parameters were chosen to be $m_1 = m_2 = 10$ kg, $m_r = 1$ kg, $k_r = 1.4$ N/m, and $\alpha_r = 2.8$ s, which corresponding to the natural frequency $\omega_n = 0.5$ rad/s and the damping coefficient $\zeta = 0.707 (\approx 1/\sqrt{2})$ of the flexible mode.

Nonminimum phase nature of the example: We note that the nonminimum phase nature of the model can be attributed to the off-diagonal terms in the mass matrix $[M^r]$ (associated with the flexible rod) in Eq. (40); setting the off-diagonal terms in the mass matrix $[M^r]$ to zero results in a minimum-phase model. A mass matrix that captures the nondiagonal terms of the mass matrix is referred to as a consistent mass matrix (as opposed to the diagonal mass matrix obtained for the two-mass/spring/damper model); such consistent models of flexible structures with noncollocated sensors and actuators capture the nonminimum-phase nature of the dynamics.[22]

B. State-Space Model

The state of the system is defined as $x = [x_1 \;\; x_2 \;\; x_3 \;\; x_4]^T$, where x_3 and x_4 represent the velocities of masses m_1 and m_2, respectively.

1. Continuous-Time State-Space Equations

The system in Eq. (40) can be represented in a state-space form as

$$\dot{x}(t) = \left[\begin{array}{cc|cc} 0 & 0 & 1 & 0 \\ 0 & 0 & 0 & 1 \\ \hline -\{[M^T]^{-1}[K_r]\} & & -\{[M^T]^{-1}[C_r]\} & \end{array}\right] x(t) + \begin{bmatrix} 0 \\ 0 \\ [M^T]^{-1} \begin{bmatrix} 0 \\ 1 \end{bmatrix} \end{bmatrix} u(t)$$

$$= \begin{bmatrix} 0 & 0 & 1 & 0 \\ 0 & 0 & 0 & 1 \\ -0.1273 & 0.1273 & -0.3564 & 0.3564 \\ 0.1273 & -0.1273 & 0.3564 & -0.3564 \end{bmatrix} x(t) + \begin{bmatrix} 0 \\ 0 \\ -0.0070 \\ 0.0839 \end{bmatrix} u(t)$$

$$y(t) = [1 \quad 0 \quad 0 \quad 0] x(t) \tag{41}$$

where $[M^T] = [M^l] + [M^r]$. The continuous-time model has two zeros at -0.3295 and 4.2495 and is nonminimum phase.

2. Sampled-Data Discrete-Time Model

The equivalent discrete-time model obtained using ZOH discretization with a sampling period of 0.01 s can expressed as

$$x(k+1) = Ax(k) + Bu(k)$$

$$y(k) = Cx(k) = [1 \quad 0 \quad 0 \quad 0] x(k) \tag{42}$$

where

$$A = \begin{bmatrix} 1 & 0 & 0.0100 & 0 \\ 0 & 1 & 0 & 0.0100 \\ -0.0013 & 0.0013 & 0.9964 & 0.0036 \\ 0.0013 & -0.0013 & 0.0036 & 0.9964 \end{bmatrix}$$

$$B = \begin{bmatrix} -0.0034 \\ 0.0419 \\ -0.6831 \\ 8.3754 \end{bmatrix} \times 10^{-4}$$

The discrete-time system [Eq. (42)] has three zeros and four states; therefore, the delay order is $r = 1$. The discretized model [Eq. (42)] is nonminimum phase [as is the continuous-time model in Eq. (41)]; however, the discretized model exhibits an additional zero as a result of the sampling process.[24]

C. Comparison of SST and OOT Approaches

During the simulations, the goal is to move the output (i.e., the displacement of the mass m_1 on the right side of the rod) from an initial value $\underline{y} = 0$ to a final value $\bar{y} = 1$; the equilibrium rigid-body configurations for the output transitions were chosen to be

$$\underline{x} = [0 \quad 0 \quad 0 \quad 0]^T \qquad \text{and} \qquad \bar{x} = [1 \quad 1 \quad 0 \quad 0]^T \qquad (43)$$

the output transition started at time $t_i = 10$ s and was completed at time $t_f = 20$ s (i.e., the length of the output-transition time interval was 10 s).

1. SST Solution

The standard optimal control can be obtained from Eq. (7) as (see Figs. 3 and 4)

$$u^*_{\text{sst}}(k) = B^T (A^T)^{k_f - k - 1} G^{-1}_{k_i, k_f} [\bar{x} - \underline{x}], \qquad k_i \le k < k_f$$
$$= 0, \qquad \text{otherwise} \qquad (44)$$

where the controllability grammian is

$$G_{k_i,k_f} = \begin{bmatrix} 45.4173 & 48.7412 & 7.4544 & 5.9133 \\ 48.7412 & 54.3389 & 8.8793 & 7.3388 \\ 7.4544 & 8.8793 & 1.6357 & 1.3344 \\ 5.9133 & 7.3388 & 1.3344 & 1.6126 \end{bmatrix} \times 10^{-4}$$

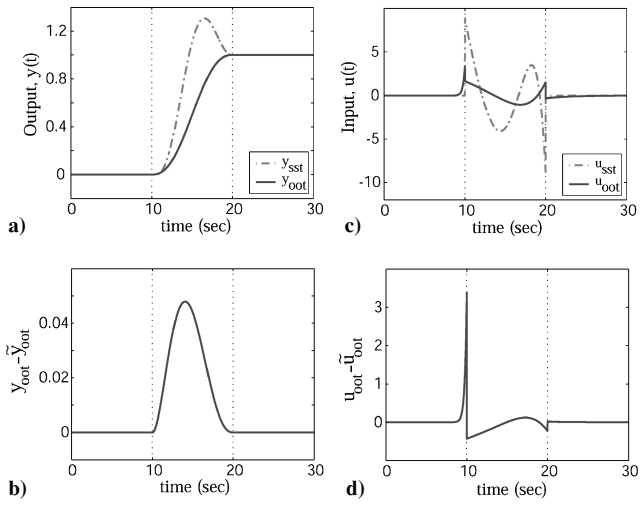

Fig. 3 Comparison of input and output trajectories for the two-mass/flexible-rod system. Figures a) and c) compare the result between using the standard state-transition approach ($u_{\text{sst}}, y_{\text{sst}}$) with the optimal output-transition approach ($u_{\text{oot}}, y_{\text{oot}}$). Figures b) and d) show the differences in the input and output ($u_{\text{oot}} - \tilde{u}_{\text{oot}}, y_{\text{oot}} - \tilde{y}_{\text{oot}}$) when using the optimal output transition with and without preactuation.

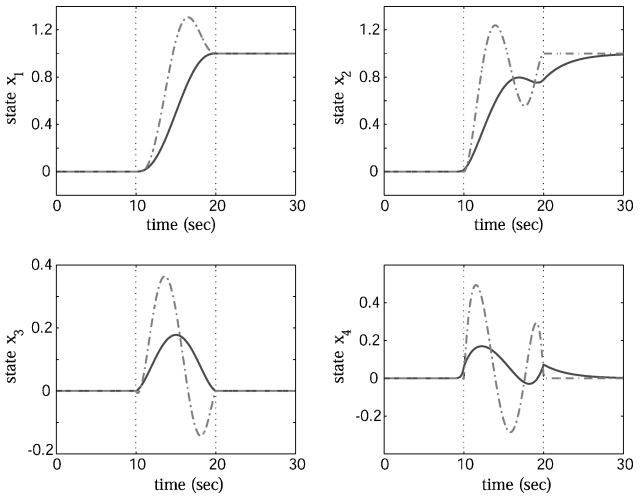

Fig. 4 Comparison of state trajectories for two-mass/flexible-rod system: - - - -, SST and ——, OOT.

the initial transition time step $k_i = 1000$ (i.e., $t_i = 10$ s) and the final transition time step $k_f = 2000$ (i.e., $t_f = 20$ s). The standard optimal cost obtained from Eq. (10) is

$$J^*_{\text{sst}} = 12{,}214.41 \qquad (45)$$

2. OOT Solution

System equations in output-tracking form. The system equations [Eq. (42)] were rewritten in the output-tracking form with decoupled internal dynamics by using the following transformation:

$$T_{\xi\eta} = \begin{bmatrix} 1 & 0 & 0 & 0 \\ 0 & 0.9771 & -2.7593 & -0.2299 \\ 0 & 0.0001 & -12.0380 & 0.0002 \\ 0 & -0.3141 & -11.4372 & -0.9533 \end{bmatrix}$$

and the control law from Eq. (19) has the form $u_{\text{inv}}(k) = U_s \eta_s(k) + U_u \eta_u(k) + U_y \mathbb{Y}_d(k)$, where $U_s = [1.34 \quad -2356.87]$, $U_u = -54.9332$, $U_y = [2.9048 \quad -2.9048] \times 10^6$, and $\mathbb{Y}_d(k) = [y_d(k) \quad y_d(k+1)]^T$. Then the system in the output-tracking coordinates is given by [similar to Eqs. (16) and (18)]

$$\xi(k+1) = y_d(k+1)$$

$$\begin{bmatrix} \eta_s(k+1) \\ \eta_u(k+1) \end{bmatrix} = \left[\begin{array}{cc|c} 0.9967 & 0 & 0 \\ 0 & -0.9847 & 0 \\ \hline 0 & 0 & 1.0434 \end{array}\right] \begin{bmatrix} \eta_s(k) \\ \eta_u(k) \end{bmatrix}$$
$$+ \left[\begin{array}{cc} 0 & 0 \\ 2.3891 & -2.3891 \\ \hline -0.0535 & 0.0535 \end{array}\right] \times 10^3 \mathbb{Y}_d(k)$$

Cost for optimal output transition. Solving the discrete Lyapunov equations (23) and (27) yields

$$W_{\text{pre}} = 34018.96 \qquad \text{and} \qquad W_{\text{post}} = \begin{bmatrix} 272.58 & -1591.46 \\ -1591.46 & 182671780.33 \end{bmatrix}$$

From Theorem 1, the optimal boundary condition Ψ can be obtained as [see Eq. (33)]

$$\Psi^* = \begin{bmatrix} \eta^*_s \\ \eta^*_u \end{bmatrix} = \Lambda^{-1} b = \begin{bmatrix} 0.74382 \\ 0.00004 \\ -0.06442 \end{bmatrix}$$

and the corresponding optimal boundary transition states are [see Eq. (35)]

$$x^*(k_i) = [0 \quad 0.0148 \quad 8.58e{-}7 \quad 0.0627]^T$$
$$x^*(k_f) = [1 \quad 0.7784 \quad 9.91e{-}7 \quad 0.0730]^T$$

Optimal output-transition control. The optimal control can be found from Eq. (34) as (see Figs. 3 and 4)

$$u^*_{\text{oot}}(k) = \begin{cases} -54.9332 \cdot (1.0434)^{k-k_i}\left[\eta^*_u - \underline{\eta_u}\right] & \text{if} \quad k < k_i \\ B^T (A^T)^{k_f-k-1} G^{-1}_{k_i,k_f}\left[x^*(k_f) - A^{k_f-k_i} x^*(k_i)\right] & \text{if} \quad k_i \le k < k_i \\ [1.34 - 2356.87] \begin{bmatrix} 0.9967 & 0 \\ 0 & -0.9847 \end{bmatrix}^{k-k_f} \left[\eta^*_s - \overline{\eta_s}\right] & \text{if} \quad k \ge k_f \end{cases} \tag{46}$$

The total cost for optimal input is found from Eq. (32) as

$$J^*_{\text{oot}} = 877.23 \tag{47}$$

3. Comparison of SST and OOT Costs

In general, the OOT cost is expected to be less than or equal to the SST cost when the output-transition time interval (i.e., time during which the output is changing) is the same for both approaches (see Remark 6). Specifically, the simulation results show that the cost required to achieve the output transition (moving the mass m_1 to the right by 1 m) using the OOT approach is $J^*_{\text{oot}} = 877.23$, whereas the cost with the SST approach was $J^*_{\text{sst}} = 12214.41$. This represents a substantial cost reduction of 93% by using the proposed OOT approach when compared to the SST approach. Although the time during which the output is changing is the same for both SST and OOT approaches, the state is not required to remain constant outside the output-transition time interval with the OOT method. For example, as shown in Fig. 4 the configuration of mass m_2 (i.e., state x_2) does not reach the equilibrium value at the end of output transition; however, the system (and the state x_2) is eventually driven to the final equilibrium state $\bar{x}$ by the inversion-based postactuation input while keeping the output (position of mass m_1) constant in order to satisfy the output-transition condition [Eq. (3)]. Thus, the OOT approach uses pre- and postactuation to reduce the input energy needed for output transition when compared to the SST approach; however, the time available for useful operation is the same as the SST approach because the output is maintained constant outside of the output-transition time interval.

D. Optimal Output Transition Without Preactuation

The proposed approach uses pre- and postactuation to achieve the minimum-energy output transition. If preactuation input is not allowed (e.g., when immediate output transition is desired), then the energy for output transition can be reduced by using postactuation alone (without preactuation).

1. OOT with and Without Preactuation

When preactuation is not allowed, the optimal output-transition input is given by [see Eq. (39)]

$$\tilde{u}^*_{\text{oot}}(k) = \begin{cases} 0 & \text{if} \quad k < k_i \\ B^T (A^T)^{k_f-k-1} G^{-1}_{k_i,k_f}\left[x^*(k_f) - \underline{x}\right] & \text{if} \quad k_i \le k < k_i \\ [1.34 - 2356.87] \begin{bmatrix} 0.9967 & 0 \\ 0 & -0.9847 \end{bmatrix}^{k-k_f} \left[\tilde{\eta}^*_s(k_f) - \overline{\eta_s}\right] & \text{if} \quad k \ge k_f \end{cases} \tag{48}$$

where the optimal stable component $\tilde{\eta}^*_s(k_f)$ of the internal dynamics is [from Eq. (38)],

$$\tilde{\eta}^*_s(k_f) = \tilde{\Lambda}^{-1}\tilde{b} = \begin{bmatrix} 0.72967 \\ 0.00004 \end{bmatrix}$$

and the optimal final boundary condition on the state is $\tilde{x}^*(k_f) = [1 \ 0.7650 \ 1.12e{-}6 \ 0.0774]^T$. The total cost for optimal output control without preactuation [Eq. (37)] is equal to

$$\tilde{J}^*_{\text{oot}} = 1055.04 \tag{49}$$

Even without preactuation, the cost $\tilde{J}^*_{\text{oot}} = 1055.04$ with the proposed optimal output-transition approach is substantially smaller than the output-transition cost $J^*_{\text{sst}} = 12214.41$ with the SST approach. In fact, it is always true that the optimal cost of the OOT without preactuation cannot be greater than the SST cost, by similar argument as described in Remark 6.

2. Effect of Preactuation Input in Systems with Minimum-Phase Dynamics

The preactuation input is affected by the nonminimum-phase zeros of the system; in discrete-time models such nonminimum-phase zeros can arise from the discretization process.[24] In such cases with fast sampling, the use of OOT inputs without preactuation cannot significantly change the cost when compared to the case with the use of the preactuation. For example, consider the flexible system [Eq. (40)] when the mass-matrix coefficient of the rod m_r [in Eq. (40)] is equal to zero; the resulting continuous-time system is minimum phase. In fact, it is equivalent to the benchmark two-mass/spring/damper system,[8,9] where the coefficients k_r and c_r can be regarded as the effective spring constant and effective damping constant, respectively. However, the sampled-data discrete-time model of this two-mass/spring/damper model is nonminimum-phase caused by the discretization process (see Ref. 24).

Comparison of SST and OOT results. The SST input [Eq. (7)] for this minimum-phase two-mass/spring/damper model [obtained by setting the mass-matrix parameter $m_r = 0$ in Eq. (40)] is given by (see Fig. 5)

$$u^*_{\text{sst}}(k) = \bar{B}^T (\bar{A}^T)^{k_f-k-1} \bar{G}^{-1}_{k_i,k_f}[\bar{x} - \underline{x}], \qquad k_i \le k < k_f$$
$$= 0, \qquad \text{otherwise} \tag{50}$$

and the OOT input using both pre- and postactuation is (see Fig. 5)

$$u^*_{\text{oot}}(k) = \begin{cases} 4733.3993 \cdot (-3.7281)^{k-k_i} \cdot (-9.3239 \times 10^{-4}) & \text{if} \quad k < k_i \\ \bar{B}^T (\bar{A}^T)^{k_f-k-1} \bar{G}^{-1}_{k_i,k_f} [0.9953 \quad 0.8038 \quad -0.0005 \quad 0.0670]^T & \text{if} \quad k_i \le k < k_i \\ [1.1991 \quad -1266.2237] \begin{bmatrix} 0.9964 & 0 \\ 0 & -0.2677 \end{bmatrix}^{k-k_f} \begin{bmatrix} -0.2034 \\ -0.0009 \end{bmatrix} & \text{if} \quad k \ge k_f \end{cases} \tag{51}$$

where the matrices $\bar{A}$, $\bar{B}$, and $\bar{G}_{k_i,k_f}$ are given by

$$\bar{A} = \begin{bmatrix} 1 & 0 & 0.01 & 0 \\ 0 & 1 & 0 & 0.01 \\ -0.0014 & 0.0014 & 0.9961 & 0.0039 \\ 0.0014 & -0.0014 & 0.0039 & 0.9961 \end{bmatrix}$$

$$\bar{B} = \begin{bmatrix} 0.0000 \\ 0.0050 \\ 0.0020 \\ 0.9980 \end{bmatrix} \times 10^{-4}$$

and

$$\bar{G}_{k_i,k_f} = \begin{bmatrix} 0.0078 & 0.0083 & 0.0013 & 0.0011 \\ 0.0083 & 0.0089 & 0.0014 & 0.0012 \\ 0.0013 & 0.0014 & 0.0003 & 0.0002 \\ 0.0011 & 0.0012 & 0.0002 & 0.0003 \end{bmatrix}$$

If preactuation is not allowed, then the OOT input without the preactuation, for the two-mass/spring/damper model, is given by

$$\tilde{u}^*_{\text{oot}}(k) = \begin{cases} 0 & \text{if} \quad k < k_i \\ \bar{B}^T (\bar{A}^T)^{k_f-k-1} \bar{G}^{-1}_{k_i,k_f} [1.0000 \quad 0.8083 \quad 0.0000 \quad 0.0675]^T & \text{if} \quad k_i \le k < k_i \\ [1.1991 \quad -1266.2237] \begin{bmatrix} 0.9964 & 0 \\ 0 & -0.2677 \end{bmatrix}^{k-k_f} \begin{bmatrix} -0.2036 \\ -0.0009 \end{bmatrix} & \text{if} \quad k \ge k_f \end{cases} \tag{52}$$

The cost of using the OOT input without the preactuation is $\tilde{J}^*_{\text{oot}} = 661.31$, which is similar to the OOT input cost $J^*_{\text{oot}} = 659.79$ with both pre- and postactuation. However, both OOT-input costs (with and without preactuation) are still substantially smaller than the SST input cost $J_{\text{sst}} = 6458.29$. [It is noted that the difference between the optimal output trajectory with preactuation input y_{oot} and without preactuation $\tilde{y}_{\text{oot}}$ is also relatively small (see Fig. 5).] In contrast, if the continuous-time system is nonminimum phase [Eq. (40)], then preactuation can significantly reduce the cost of output transition when compared to the case without the preactuation. For example, in the flexible-rod coupling case the output-transition cost $\tilde{J}^*_{\text{oot}} = 1055.04$ [Eq. (49)] without preactuation was substantially higher when compared to the cost $J^*_{\text{oot}} = 877.23$ [Eq. (47)] with preactuation. Thus, the preactuation input plays a significant role in reducing the output-transition cost with the proposed OOT approach when the continuous-time dynamics is nonminimum phase.

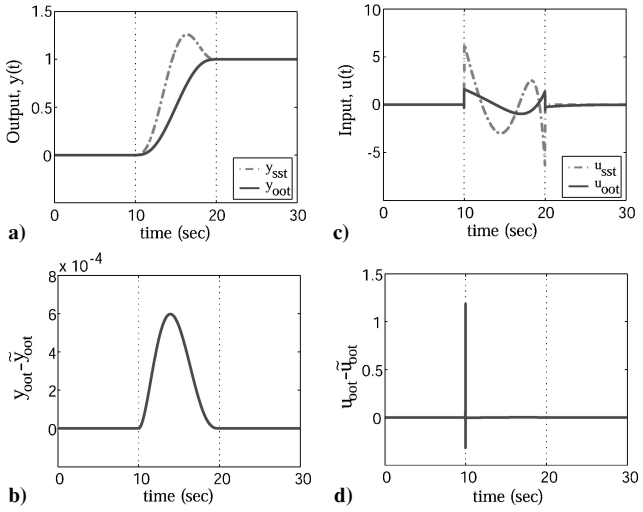

Fig. 5 Comparison of input and output trajectories when setting the mass of flexible rod $m_r = 0$ (which is equivalent to a two-mass/spring/damper system). Figures a) and c) compare the input and output ($u_{\text{sst}}, y_{\text{sst}}$) from the standard state-transition approach with those from the optimal output-transition approach ($u_{\text{oot}}, y_{\text{oot}}$). Figures b) and d) show the differences in the input and output ($u_{\text{oot}} - \tilde{u}_{\text{oot}}, y_{\text{oot}} - \tilde{y}_{\text{oot}}$) when using optimal output transition with and without preactuation.

E. Effect of Varying the Output-Transition Time Interval

The proposed approach can be used to investigate the fastest achievable output-transition time for a given limit on the input energy. For the flexible-rod example, the input energy is plotted against the output-transition time (with the OOT and SST approaches) in Fig. 6. Additionally, the variation in the maximum input magnitude ($\max_k |u(k)|$), when the output-transition time interval ($t_f - t_i$) is varied, is also shown in Fig. 6. As shown in the Fig. 6, the input energy (for both SST and OOT approaches) increases as the output-transition time decreases. The simulation results show that, for a given output-transition time, the cost for OOT input is an order of

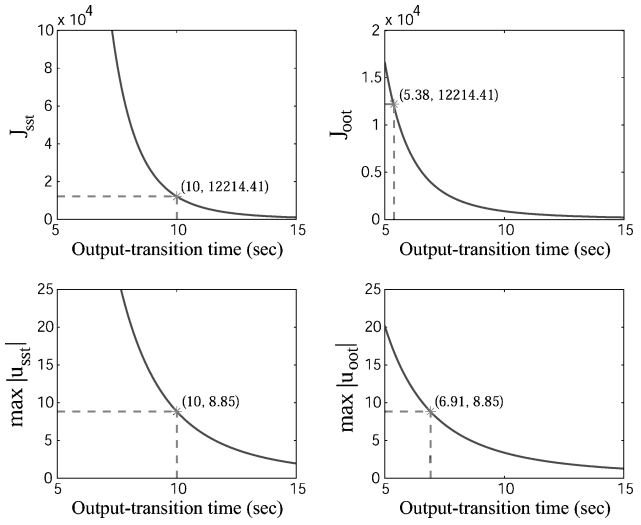

Fig. 6 Comparison of the optimal cost and maximum input magnitude between SST and OOT when the output-transition time interval ($k_f - k_i$) is varied for the two-mass/flexible-rod example where $\max|u_{\text{sst}}| = \max_k|u_{\text{sst}}(k)|$ and $\max|u_{\text{oot}}| = \max_k|u_{\text{oot}}(k)|$.

Table 1 Effect of the damping ratio on the output-transition costs for the flexible structure example

ζ	α_r	J_{sst}	J_{oot}	$\%\Delta J$	J_{pre}	$\frac{J_{\text{pre}}}{J_{\text{oot}}}$, %	J_{post}	$\frac{J_{\text{post}}}{J_{\text{oot}}}$, %	$\tilde{J}_{\text{oot}}$	$\%\Delta J_{\tilde{u}_{\text{oot}}}$
0.01	0.04	6,068.96	681.98	88.76	298.83	43.82	292.92	42.95	1,820.66	70.00
0.1	0.4	6,201.04	690.91	88.86	305.27	44.18	248.24	35.93	1,506.45	75.71
0.2	0.8	6,598.76	715.90	89.15	282.46	39.46	180.15	25.16	1,287.92	80.48
0.3	1.2	7,253.69	751.04	89.65	247.01	32.89	117.20	15.60	1,167.92	83.90
0.4	1.6	8,155.28	789.06	90.32	212.40	26.92	71.44	9.05	1,107.35	86.42
0.5	2.0	9,291.07	824.32	91.13	183.31	22.24	42.31	5.13	1,078.07	88.40
0.6	2.4	10,648.18	853.93	91.98	159.93	18.73	24.94	2.92	1,063.48	90.01
0.707	2.8	12,214.41	877.23	92.82	141.19	16.09	14.85	1.69	1,055.04	91.36
0.8	3.2	13,979.00	894.79	93.60	125.99	14.08	9.00	1.01	1,048.78	92.50
0.9	3.6	15,932.88	907.53	94.30	113.46	12.50	5.57	0.61	1,043.02	93.45
1.0	4.0	18,068.70	916.46	94.93	102.98	11.24	3.53	0.39	1,037.18	94.26

magnitude lower than the cost for SST input as shown in Fig. 6; this is expected (see Remark 6). This implies that the OOT approach can achieve faster output transition than the SST approach with the same amount of input energy. For example, in the nominal flexible-rod system the cost required for 10-s output-transition time is $J^*_{\text{sst}} = 12214.41$ when using the SST approach; however, with the same amount of input energy the output transition using OOT approach can be done within 5.38 s. Additionally, the maximum input magnitude of the OOT input is also less than that of the SST input. In particular, with a 10-s output-transition time, the maximum input magnitude of the SST input is 8.85; the output transition using OOT approach could be achieved in 6.91 s with the same magnitude of maximum input. Thus, the proposed approach tends to achieve significantly faster output transitions when compared to the SST approach.

F. Effects of Damping-Ratio Variation

Changes in the system damping affect the decay rate of residual vibrations after the end of an output transition. For example, vibrations tend to decay faster as the damping is increased; thus, it might be possible that the proposed use of postactuation might not lead to significant cost savings for highly damped systems. Therefore, we investigated the effect of damping on the output-transition cost. In particular, we computed the SST and OOT inputs and comparatively evaluated the input costs for different values of the system's damping ratio of the flexible mode (without changing the natural frequency). Table 1 tabulates the SST cost J_{sst} [Eq. (10)], the OOT cost J_{oot} [Eq. (36)], the percentage reduction of cost

$$\%\Delta J := (J_{\text{sst}} - J_{\text{oot}})/J_{\text{sst}} \times 100 \tag{53}$$

the preactuation cost J_{pre} [Eq. (21)], and the postactuation cost J_{post} [Eq. (25)] for different values of damping ratio of the flexible mode (achieved by changing the damping factor α_r). Additionally, to compare the relative importance of pre- and postactuation the table provides the percentage ratios of the preactuation cost and postactuation cost to the total output-transition cost J_{oot} [Eq. (36)]. Lastly, the OOT cost without preactuation $\tilde{J}_{\text{oot}}$ [Eq. (37)], and the percentage reduction of cost when using the OOT input without the preactuation

$$\%\Delta J_{\tilde{u}_{\text{oot}}} := (J_{\text{sst}} - \tilde{J}_{\text{oot}})/J_{\text{sst}} \times 100 \tag{54}$$

at different values of the damping ratios are also presented in Table 1.

The simulation results show that the cost savings (because of the use of pre- and postactuation in the OOT input) increases as the damping ratio increases. When the damping ratio is increased, the SST cost J_{sst} increases while the OOT cost J_{oot} decreases, as shown in Table 1. Thus, an increase in damping ratio still leads to substantial reduction in the output-transition costs with the use of the OOT input when compared to the results of using the SST input.

We note that the pre- and postactuation inputs, given in Eqs. (20) and (24), depend on the internal dynamics [Eq. (18)] of the original system, which is influenced by the system's zeros as described in Sec. IV.A.2. In the flexible-rod system, the continuous-time zero tends to move away from the imaginary axis (for underdamped systems); therefore, the corresponding discrete-time zero tends to move towards the origin. Consequently, the postactuation input [Eq. (24)] decays faster as the damping is increased because the internal dynamics [Eq. (18)], which depend on the system's zeros, decays faster when the zeros are further away from the unit circle (i.e., are closer to the origin). Faster decay of the the postactuation input implies that the cost of postactuation decreases as the damping is increased (see column 8 in Table 1); nevertheless, the postactuation still leads to a substantial reduction in the overall cost when compared to the SST case, which does not use postactuation (compare columns 3 and 4 in Table 1).

G. Sensitivity of the Optimal Control to the Modeling Uncertainties

1. *Effect of Parametric Uncertainties*

Information about the system model is used to compute the optimal transition controls (both SST and OOT); therefore, parametric uncertainties in the model can affect the performance of the proposed control strategies. We studied the effect of parametric uncertainties by applying the the nominal SST input [Eq. (44)] and nominal OOT input [Eq. (46)] to perturbed models of the system and then evaluating the effect of the perturbations on the performance. It is noted that robustness of control laws for flexible structure applications has been studied in the past by varying the damping ratio and natural frequency of the flexible vibrational modes (e.g., Refs. 3, 8, and 16). Following this approach, the flexible structure model was perturbed by varying the stiffness coefficient k_r and by varying the damping factor α_r. The performance of the nominal SST and OOT inputs (when applied to the perturbed models) was measured by computing the maximum percentage error in the position during pre- and postactuation, that is, the error in the output outside of the output-transition time interval as a percentage of the change in the desired output value $(\bar{y} - \underline{y})$,

$$\%e_y := \max_{k \le k_i \text{ and } k \ge k_f} \left| \frac{y(k) - y_{\text{nom}}(k)}{\bar{y} - \underline{y}} \times 100 \right| \tag{55}$$

where $y_{\text{nom}}(k)$ is the nominal output trajectory. Simulation results are provided when the nominal SST input [Eq. (44)] and the nominal OOT input [Eq. (46)] were applied to the system for the following cases: 1) stiffness coefficient k_r, was varied from 0 to $\pm 20\%$ of the nominal value of 1.4 N/m (Fig. 7a); and 2) the damping factor α_r, was varied from 0 to $\pm 20\%$ of the nominal value 2.8 s (Fig. 7b). The effect of variations in the stiffness coefficient k_r and the damping factor α_r to the changes in natural frequency ω_n and the damping ratio ζ of the flexible mode are presented in Figs. 7c and 7d, respectively.

As shown in Fig. 7, the tracking error $\%e_y$ of the OOT input to the parametric uncertainties is less than 4% when the stiffness coefficient k_r is varied by $\pm 20\%$ of its original value, and the tracking error was also less than 4% when the damping factor α_r is varied by $\pm 20\%$ of its original value. Thus the tracking error with the OOT input remained less than 4% when the parameters varied by 20%—this is similar to the tracking errors obtained when the SST input was applied to the perturbed system as seen in Fig. 7.

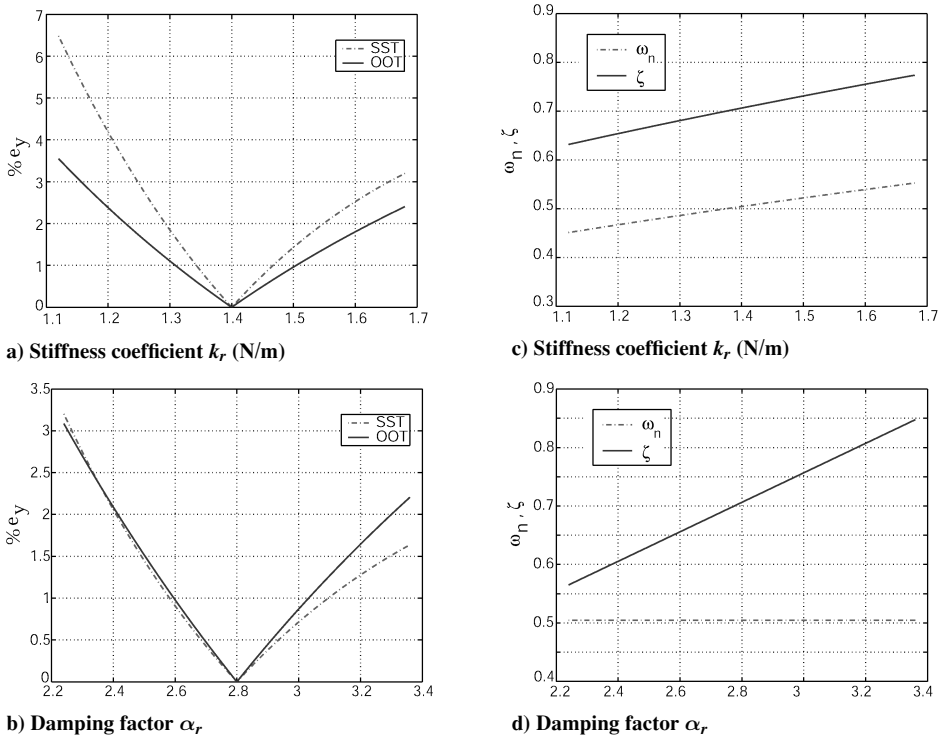

a) Stiffness coefficient k_r (N/m)

c) Stiffness coefficient k_r (N/m)

b) Damping factor α_r

d) Damping factor α_r

Fig. 7 Percentage of maximum difference between the output trajectory and the nominal output trajectory outside the transition time interval $\%e_y$ when a) the stiffness coefficient k_r is varied and b) the damping factor α_r is varied, and the effects to the natural frequency ω_n and the damping ratio ζ of the flexible mode when c) k_r is varied while α_r is fixed at the nominal value and d) α_r is varied while k_r is fixed at the nominal value.

Table 2 Output error [$\%e_y$ defined in Eq. (55)] found using simulations when the number of elements in the FEM model was changed from one to six

No. of elements	$\%e_y$ with SST input	$\%e_y$ with OOT input
(Nominal) 1	0	0
2	0.0710	0.0457
3	0.0645	0.0607
4	0.0610	0.0665
5	0.0592	0.0692
6	0.0592	0.0707

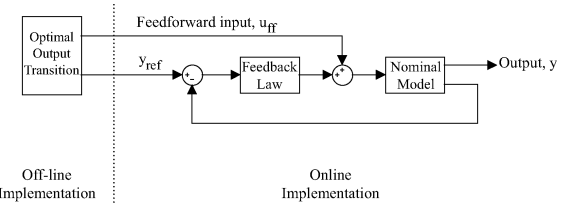

Fig. 8 Block diagram of a feedforward/feedback implementation scheme. The optimal output-transition input u_{oot} can be computed offline and applied to the system as a feedforward input $u_{ff} = u_{oot}$.

2. Effect of Nonparametric Uncertainties

When designing controllers for flexible structures, high-frequency vibrational modes are often neglected in order to obtain a simplified model. For example, the flexible rod used in this simulation has infinite vibrational modes. However, it was modeled using a simplified one-element finite element model (FEM) [Eq. (40)], which approximately captures the first flexible (vibrational) mode of the rod. Therefore, nonparametric uncertainties (such as the effect of unmodeled vibrational dynamics) can affect the performance of the proposed control strategies. We studied the effect of nonparametric uncertainties by applying the the nominal SST input [Eq. (44)] and the nominal OOT input [Eq. (46)] to perturbed models of the system. Perturbed models were obtained by increasing the number of FEM elements used for modeling the flexible rod. The performance of the nominal SST and OOT inputs (when applied to the perturbed models) was measured by computing the maximum percentage error in the position during pre- and postactuation $\%e_y$ as defined in Eq. (55). Table 2 shows the effects of nonparametric uncertainties found using simulations when the number of elements in the FEM model was changed from one to six. As shown in Table 2, the tracking error remains negligible for this example (less than 0.1%) as the number of FEM elements is increased from one to six.

3. Use of Feedback with the Proposed OOT Approach

In all of these simulations, the SST and OOT inputs were applied as the open-loop feedforward input to the perturbed system without feedback. The performance of the OOT input (in the presence of parametric and nonparametric uncertainties) can be further improved with the use of robust feedback control techniques; as shown in Fig. 8, the OOT input can be used as a feedforward input along with a feedback controller. Moreover, the effect of nonparametric uncertainties in the flexible structure can be mitigated by the use of spillover control techniques (for example, see Ref. 25). The use of feedforward inputs (such as the OOT input computed using the nominal plant) can improve the tracking performance when compared to the use of feedback alone even in the presence of plant uncertainties. (The size of acceptable uncertainties has been quantified in Ref. 26.)

In summary, the simulation results show that the proposed approach performs well (in comparison to more established techniques such as the state-transition-based approach) in the presence of uncertainties (even without the use of feedback)—and does so with a lower cost for the transition.

VI. Conclusions

The optimal rest-to-rest output-transition problem was solved in this paper, for linear time-invariant discrete-time systems. The novelty of the proposed approach is that inputs are not applied just during the output-transition time interval; rather, inputs are also applied before and after the end of the output-transition time interval. (These inputs are called pre- and postactuation, respectively.) It was shown that this approach of using pre- and postactuation inputs can substantially reduce the overall cost of the output-transition when compared to current approaches, such as the standard state-transition

(SST) approach, which does not use pre- and postactuation. The implications of using (or not using) pre- and postactuation were investigated using a discrete-time flexible-structure model consisting of a flexible rod connecting two masses. The simulation results showed that the proposed approach reduces the output-transition cost by 93%. Thus, the proposed use of pre- and postactuation led to substantial reduction in output-transition cost when compared to the SST approach. This concept of using pre- and postactuation to reduce the transition cost is general and can be extended to nonlinear systems and can be applied with other optimization criteria.

Appendix: Proof of Lemma 2

It is assumed that the original system [Eq. (1)] is already transformed into the output-tracking form by using the inversion-based control law [Eq. (13)] and the coordinate transformation $T_{\xi\eta}$, given in Eq. (14).

Because the output along the pretransition interval ($k \le k_i - r$) is constant [see Eq. (3)], i.e., $y(k) = \underline{y}$, the output-sequence vector $\mathbb{Y}_d(k)$, defined in Sec. IV.A.2, becomes

$$\mathbb{Y}_d(k) = \underline{\mathbb{Y}} := [\underline{y} \quad \underline{y} \quad \dots \quad \underline{y}] \qquad \forall k \in (-\infty, k_i - r] \quad \text{(A1)}$$

As described in Sec. IV.A.1, the inversion-based control yields the exact output tracking with r-step time delay. Therefore, the output obtained by applying the inverse control law [Eq. (19)] satisfies the output-transition condition [Eq. (3)] during the pretransition, that is, $y(k) = \underline{y}, \forall k \le k_i - r$. Next, we consider the output-tracking coordinates (ξ and η) corresponding to the initial delimiting state ($\underline{x}$),

$$\begin{bmatrix} \underline{\xi} \\ \underline{\eta}_s \\ \underline{\eta}_u \\ \underline{\eta}_c \end{bmatrix} := T_{\xi\eta}\underline{x}$$

where the transformation $T_{\xi\eta}$ is given in Eq. (14). The internal dynamics [Eq. (18)] evaluated at the equilibrium state $\underline{x}$ is then expressed as

$$\begin{bmatrix} \underline{\eta}_s \\ \underline{\eta}_u \\ \underline{\eta}_c \end{bmatrix} = \begin{bmatrix} A_s & 0 & 0 \\ 0 & A_u & 0 \\ 0 & 0 & A_c \end{bmatrix} \begin{bmatrix} \underline{\eta}_s \\ \underline{\eta}_u \\ \underline{\eta}_c \end{bmatrix} + \begin{bmatrix} B_s \\ B_u \\ B_c \end{bmatrix} \underline{\mathbb{Y}} \qquad \text{(A2)}$$

To simplify the derivation, the coordinates of the internal dynamics are shifted as $\hat{\eta}(k) = \eta(k) - \underline{\eta}$ by subtracting the internal dynamics [Eq. (18)] from Eq. (A2) and using the equality (A1). Thus the modified internal dynamics can be written as

$$\begin{bmatrix} \hat{\eta}_s(k+1) \\ \hat{\eta}_u(k+1) \\ \hat{\eta}_c(k+1) \end{bmatrix} = \begin{bmatrix} A_s & 0 & 0 \\ 0 & A_u & 0 \\ 0 & 0 & A_c \end{bmatrix} \begin{bmatrix} \hat{\eta}_s(k) \\ \hat{\eta}_u(k) \\ \hat{\eta}_c(k) \end{bmatrix} \qquad \text{(A3)}$$

Furthermore, because the internal dynamics [Eq. (A3)] can be singular, it can be assumed without loss of generality that the stable internal dynamics $\hat{\eta}_s$ is decoupled into singular $\hat{\eta}_{s_s}$ and nonsingular $\hat{\eta}_{s_{\text{ns}}}$ stable subspaces, that is,

$$A_s := \begin{bmatrix} A_{s_s} & 0 \\ 0 & A_{s_{\text{ns}}} \end{bmatrix} \qquad \text{and} \qquad \hat{\eta}_s := \begin{bmatrix} \hat{\eta}_{s_s} \\ \hat{\eta}_{s_{\text{ns}}} \end{bmatrix}$$

where all of the eigenvalues of A_{s_s} are at the origin.

For a given initial transition state $x(k_i - r + 1)$, the solution to the internal dynamics [Eq. (A3)] at time step k can be expressed as

$$\hat{\eta}_{s_{\text{ns}}}(k) = A_{s_{\text{ns}}}^{-(k_i - k - r + 1)} \hat{\eta}_{s_{\text{ns}}}(k_i - r + 1)$$

$$\hat{\eta}_u(k) = A_u^{-(k_i - k - r + 1)} \hat{\eta}_u(k_i - r + 1) \qquad \forall k \in (-\infty, k_i - r]$$

$$\hat{\eta}_c(k) = A_c^{-(k_i - k - r + 1)} \hat{\eta}_c(k_i - r + 1) \qquad \text{(A4)}$$

The delimiting condition (4) requires that, as time tends to $-\infty$ ($k \to -\infty$), the state should approach the initial equilibrium state, that is, $x(k) \to \underline{x}$ [$\hat{\eta}(k) \to 0$]. We enforce this condition by taking limits on both sides of Eq. (A4) and setting them to zero as follows:

$$0 = \lim_{k \to -\infty} \hat{\eta}_{s_{\text{ns}}}(k) = \lim_{k \to -\infty} A_{s_{\text{ns}}}^{-(k_i - k - r + 1)} \hat{\eta}_{s_{\text{ns}}}(k_i - r + 1)$$

$$0 = \lim_{k \to -\infty} \hat{\eta}_u(k) = \lim_{k \to -\infty} A_u^{-(k_i - k - r + 1)} \hat{\eta}_u(k_i - r + 1)$$

$$0 = \lim_{k \to -\infty} \hat{\eta}_c(k) = \lim_{k \to -\infty} A_c^{-(k_i - k - r + 1)} \hat{\eta}_c(k_i - r + 1) \qquad \text{(A5)}$$

Because the eigenvalues of $A_{s_{\text{ns}}}^{-1}$ and A_c^{-1} are not inside the unit circle, therefore, the delimiting condition [Eq. (4)] is satisfied if and only if

$$\hat{\eta}_{s_{\text{ns}}}(k_i - r + 1) = 0, \qquad \hat{\eta}_c(k_i - r + 1) = 0 \qquad \text{(A6)}$$

Next we consider the singular stable internal dynamics $\hat{\eta}_{s_s}$ evaluated at time step $k_i - r + 1$,

$$\hat{\eta}_{s_s}(k_i - r + 1) = A_{s_s} \hat{\eta}_{s_s}(k_i - r), \qquad \forall k \in (-\infty, k_i - r]$$

$$= A_{s_s}^{n_{s_s}} \hat{\eta}_{s_s}\left(k_i - r - n_{s_s} + 1\right) \qquad \text{(A7)}$$

where n_{s_s} is the number of eigenvalues of A_{s_s}. Because all of the eigenvalues of A_{s_s} are equal to zero, $A_{s_s}^{n_{s_s}} = 0$. Therefore,

$$\hat{\eta}_{s_s}(k_i - r + 1) = A_{s_s}^{n_{s_s}} \hat{\eta}_{s_s}\left(k_i - r - n_{s_s} + 1\right) = 0 \qquad \text{(A8)}$$

This equation and the results from Eq. (A6) also imply that

$$\hat{\eta}_s(k) = 0, \qquad \text{that is,} \qquad \eta_s(k) = \underline{\eta}_s$$

and

$$\hat{\eta}_c(k) = 0, \qquad \text{that is,} \qquad \eta_c(k) = \underline{\eta}_c \qquad \forall k \in (-\infty, k_i - r] \qquad \text{(A9)}$$

Therefore, the only freedom in the state at the initiation of output transition $x(k_i - r + 1)$ is in the choice of the unstable internal-state component $\eta_u(k_i - r + 1)$.

Preactuation Input and Cost

Note that at the equilibrium point $\underline{x}$, $A\underline{x} = \underline{x}$, so that $CA^r\underline{x} = C\underline{x} = \underline{y}$.

Therefore, the inverse control input [Eq. (13)] evaluated at the equilibrium point $\underline{x}$ is

$$u_{\text{inv}}(k)|_{x(k)=\underline{x}} = \underline{u}_{\text{inv}} := (1/CA^{r-1}B)[\underline{y} - CA^r\underline{x}] = 0$$

The inverse control input expressed in terms of internal states [Eq. (19)] at the equilibrium point is then written as

$$\underline{u}_{\text{inv}} = 0 = U_s\underline{\eta}_s + U_u\underline{\eta}_u + U_c\underline{\eta}_c + U_y\underline{\mathbb{Y}} \qquad \text{(A10)}$$

Similarly, the inverse control input represented in term of new internal coordinate $\hat{\eta}(k)$ can be obtained by subtracting the inverse control law [Eq. (19)] from Eq. (A10),

$$u_{\text{inv}}(k) = U_s[\eta_s(k) - \underline{\eta}_s] + U_u[\eta_u(k) - \underline{\eta}_u] + U_c[\eta_c(k) - \underline{\eta}_c]$$

$$= U_s\hat{\eta}_s(k) + U_u\hat{\eta}_u(k) + U_c\hat{\eta}_c(k) \qquad \text{[using Eq. (A9)]}$$

$$= U_u\hat{\eta}_u(k) \qquad \forall k \in (-\infty, k_i - r] \qquad \text{(A11)}$$

Therefore, the pretransition control sequence, which satisfies the output-transition condition [Eq. (3)] and the delimiting condition [Eq. (4)], only depends on the unstable component of internal dynamics η_u. The preactuation inverse control can be rewritten as [from Eq. (A4)]

$$u_{\text{pre}}(k) = U_u A_u^{-(k_i - k - r + 1)} \hat{\eta}_u(k_i - r + 1)$$

$$= U_u A_u^{-(k_i - k - r + 1)} [\eta_u(k_i - r + 1) - \underline{\eta}_u]$$

and the pretransition cost can be computed as

$$
\begin{aligned}
J_{\text{pre}} &= \sum_{k=-\infty}^{k_i-r} [u_{\text{pre}}(k)]^2 \\
&= \sum_{k=-\infty}^{k_i-r} \left\{ U_u A_u^{-(k_i-k-r+1)} [\eta_u(k_i-r+1) - \underline{\eta}_u] \right\}^T \\
&\quad \times \left\{ U_u A_u^{-(k_i-k-r+1)} [\eta_u(k_i-r+1) - \underline{\eta}_u] \right\} \\
&= [\eta_u(k_i-r+1) - \underline{\eta}_u]^T \left[\sum_{k=-\infty}^{k_i-r} \left(A_u^T\right)^{-(k_i-k-r+1)} \right. \\
&\quad \left. \times U_u^T U_u A_u^{-(k_i-k-r+1)} \right] [\eta_u(k_i-r+1) - \underline{\eta}_u]
\end{aligned}
$$

By defining the summation index $\bar{k} = k_i - k - r$, we can rewrite the pretransition cost as

$$
\begin{aligned}
J_{\text{pre}} &= [\eta_u(k_i-r+1) - \underline{\eta}_u]^T \left[\sum_{\bar{k}=0}^{\infty} \left(A_u^T\right)^{-(\bar{k}+1)} U_u^T U_u A_u^{-(\bar{k}+1)} \right] \\
&\quad \times [\eta_u(k_i-r+1) - \underline{\eta}_u] \\
&= [\eta_u(k_i-r+1) - \underline{\eta}_u]^T W_{\text{pre}} [\eta_u(k_i-r+1) - \underline{\eta}_u]
\end{aligned}
$$

Furthermore, the matrix W_{pre} can be obtained as a solution to the discrete-time algebraic Lyapunov equation (23) (see Ref. 27). □

Acknowledgment

Financial support from NASA Ames Research Center Grant NAG 2-1450 is gratefully acknowledged.

References

[1]Farrenkopf, R., "Optimal Open-Loop Maneuver Profiles for Flexible Spacecraft," *Journal of Guidance, Control, and Dynamics*, Vol. 2, No. 6, 1979, pp. 491–498.

[2]Singh, G., Kabamba, P., and McClamroch, N., "Planar, Time-Optimal, Rest-to-Rest Slewing Maneuvers of Flexible Spacecraft," *Journal of Guidance, Control, and Dynamics*, Vol. 12, No. 1, 1989, pp. 71–81.

[3]Wie, B., Sinha, R., and Liu, Q., "Robust Time-Optimal Control of Uncertain Flexible Spacecraft," *Journal of Guidance, Control, and Dynamics*, Vol. 15, No. 3, 1992, pp. 597–604.

[4]De Luca, A., and Di Giovanni, G., "Rest-to-Rest Motion of a One-Link Flexible Arm," *2001 IEEE/ASME International Conference on Advanced Intelligent Mechatronics Proceedings*, Vol. 2, IEEE Press, Piscataway, NJ, 2001, pp. 923–928.

[5]Miu, D., and Bhat, S., "Minimum Power and Minimum Jerk Position Control and Its Applications in Computer Disk Drives," *IEEE Transactions on Magnetics*, Vol. 27, No. 6, 1991, pp. 4471–4475.

[6]Ho, H., "Fast Servo Bang-Bang Seek Control," *IEEE Transactions on Magnetics*, Vol. 33, No. 6, 1997, pp. 4522–4527.

[7]Croft, D., and Devasia, S., "Vibration Compensation for High Speed Scanning Tunneling Microscopy," *Review of Scientific Instruments*, Vol. 70, No. 12, 1999, pp. 4600–4605.

[8]Hindle, T., and Singh, T., "Robust Minimum Power/Jerk Control of Maneuvering Structures," *Journal of Guidance, Control, and Dynamics*, Vol. 24, No. 4, 2001, pp. 816–826.

[9]Singh, T., "Fuel/Time Optimal Control of the Benchmark Problem," *Journal of Guidance, Control, and Dynamics*, Vol. 18, No. 6, 1995, pp. 1225–1231.

[10]Meckl, P., and Seering, W., "Minimizing Residual Vibration for Point-to-Point Motion," *Journal of Vibration, Acoustics, Stress, and Reliability in Design*, Vol. 107, No. 4, 1985, pp. 378–382.

[11]Piazzi, A., and Visioli, A., "Minimum-Time System-Inversion-Based Motion Planning for Residual Vibration Reduction," *IEEE/ASME Transactions on Mechatronics*, Vol. 5, No. 1, 2000, pp. 12–22.

[12]Dowd, A., and Thanos, M., "Vector Motion Processing Using Spectral Windows," *IEEE Control Systems Magazine*, Vol. 20, No. 5, 2000, pp. 8–19.

[13]Perez, H., and Devasia, S., "Optimal Output-Transitions for Linear Systems," *Automatica*, Vol. 39, No. 2, 2003, pp. 181–192.

[14]Zou, Q., and Devasia, S., "Preview-Based Stable-Inversion for Output Tracking of Linear Systems," *Journal of Dynamics Systems, Measurement and Control*, Vol. 121, No. 4, 1999, pp. 625–630.

[15]Spector, V. A., and Flashner, H., "Modeling and Design Implications of Noncollocated Control in Flexible System," *Journal of Dynamic Systems, Measurement, and Control*, Vol. 112, No. 2, 1990, pp. 186–193.

[16]Al-Masoud, N., Chu, S.-Y., and Singh, T., "Discrete Time Point-to-Point Control of Flexible Structures," *Proceedings of the American Control Conference*, Vol. 4, No. 6, American Automatic Control Council, Dayton, OH, 2000, pp. 2433–2437.

[17]Lewis, F. L., and Syrmos, V. L., *Optimal Control*, 2nd ed., Wiley, New York, 1995, Chap. 3.

[18]Isidori, A., *Nonlinear Control Systems*, 3rd ed., Springer-Verlag, London, 1995, Chap. 4, pp. 143, 144.

[19]Kotta, U., *Inversion Method in the Discrete-Time Nonlinear Control Systems Synthesis Problems*, Lecture Notes in Control and Information Sciences, Vol. 205, Springer-Verlag, London, 1995, Chaps. 3, 4.

[20]Ortega, J., *Matrix Theory*, Plenum, New York, 1987, p. 154.

[21]Wie, B., and Bernstein, D., "Benchmark Problems for Robust Control Design," *Journal of Guidance, Control, and Dynamics*, Vol. 15, No. 5, 1992, p. 1057.

[22]Moulin, H., and Bayo, E., "Accuracy of Discrete Models for the Solution of the Inverse Dynamics Problem for Flexible Arms, Feasible Trajectories," *Journal of Dynamics Systems, Measurement, and Control*, Vol. 119, No. 3, 1997, pp. 396–404.

[23]Bathe, K., *Finite Element Procedures*, Prentice–Hall, Englewood Cliffs, NJ, 1996, Chap. 5.

[24]Åström, K., Hagander, P., and Sternby, J., "Zeros of Sampled Systems," *Automatica*, Vol. 20, No. 1, 1984, pp. 31–38.

[25]Balas, M., "Active Control of Flexible Systems," *Journal of Optimiztion Theory and Applications*, Vol. 25, No. 3, 1978, pp. 415–436.

[26]Devasia, S., "Should Model-Based Inverse Inputs Be Used as Feedforward Under Plant Uncertainty?" *IEEE Transactions on Automatic Control*, Vol. 47, No. 11, 2002, pp. 1865–1871.

[27]Tippett, M., and Marchesin, D., "Bounds for Solutions of the Discrete Algebraic Lyapunov Equation," *IEEE Transactions on Automatic Control*, Vol. 44, No. 1, 1999, pp. 214–218.